A Rotor Position and Speed Observer for Permanent-Magnet Motors With Nonsinusoidal EMF Waveform

Cristian De Angelo, *Member, IEEE*, Guillermo Bossio, Jorge Solsona, *Senior Member, IEEE*, Guillermo O. García, *Senior Member, IEEE*, and María Inés Valla, *Senior Member, IEEE*

***Abstract*—A new nonlinear reduced-order observer to estimate the rotor speed and position for permanent-magnet motors, with arbitrary electromotive force (EMF) waveform, is presented. The proposed observer is suitable for the realization of a torque control with minimum torque ripple. In order to implement the observer, the EMF generated by the motor is first obtained experimentally offline. After that, it is approximated by a Fourier series in order to develop the model to be used in the online estimation. From the estimated EMF, rotor position and speed are calculated using the relationship between the EMF and the rotor variables. The proposal is validated with experimental results.**

***Index Terms*—Nonlinear estimation, nonsinusoidal electromotive force (EMF) waveform, permanent-magnet motors.**

I. Introduction

PERMANENT-MAGNET ac machines (PMACMs) are characterized by their high performance and high power density, mainly due to the presence of high-energy density magnets. One possible classification for these machines, depending on the waveform of their induced electromotive forces (EMFs), is the following [1]:

- *sinusoidal PMACMs* (sinusoidal-induced EMF, usually called permanent-magnet synchronous machines);
- *trapezoidal PMACMs* (trapezoidal-induced EMF, also known as brushless dc machines).

In both cases, the motor excitation current waveforms have to be synchronized with the rotor position in order to obtain smooth, ripple-free, motor torque. The use of absolute encoders, resolvers, or Hall sensors makes this synchronization possible. However, these sensors increase costs and reduce the drive robustness.

In order to avoid using these sensors, different methods for PMACM sensorless control, based on the measurement of electrical variables, have been investigated and developed [2].

Different observers have been proposed for sinusoidal PMACMs in order to obtain information about the rotor instantaneous position [3], [4]. They allow the machine excitation using sinusoidal currents synchronized with the rotor position in the whole cycle.

Trapezoidal PMACMs are usually excited with quasi-square-wave current waveforms with a 2/3 duty cycle. These currents only need a good synchronization every 60° electrical interval. Thus, the sensorless control algorithm needs to detect only six commutation instants per electrical cycle to generate the six-step switched current [5], [6].

However, many PMACMs present EMF waveforms that are neither sinusoidal nor trapezoidal. In this case, more than current synchronization is required to obtain a smooth, ripple-free, controlled torque. The current waveform should be shaped as a function of the EMF waveform. Several techniques have been proposed to obtain smooth torque by actively controlling the excitation current waveforms [7]. One of the most popular approaches is the *programmed current waveform control* (PCWC). It uses excitation current waveforms programmed as determined functions of the rotor position to generate the desired torque while canceling the pulsating torque components.

Since position estimation techniques for nonsinusoidal nor trapezoidal EMF machines have not been widely investigated, in previous proposals the information of the rotor position, needed by PCWC strategies, is obtained using a mechanical rotor position sensor. Therefore, the objective of this work is to design an observer that is not limited to sinusoidal or trapezoidal PMACMs, allowing the implementation of a sensorless control strategy. Thus, a new nonlinear reduced-order observer to estimate the EMF, the rotor position and the rotor speed for arbitrary EMF waveform machines is proposed. The motor model used to design the observer includes a Fourier series approximation of the EMF waveform. The proposed observer is used in this paper to implement an experimental PMACM sensorless drive, using a programmed current waveform control strategy. Experimental results demonstrate that the proposed scheme greatly

Manuscript received Augut 2, 2002; revised December 17, 2004. Abstract published on the Internet March 14, 2005. This work was supported by the Universidad Nacional de Río Cuarto (UNRC), by the Universidad Nacional de La Plata (UNLP), by the Universidad Nacional del Sur (UNS), by by FONCyT-ANPCyT and by CONICET. An earlier version of this paper was presented at the 28th Annual Conference of the IEEE Industrial Electronics Society, Seville, Spain, November 5–8, 2002.

C. De Angelo, G. Bossio, and G. O. García are with the Consejo Nacional de Investigaciones Científicas y Técnicas (CONICET), Argentina, and also with the Grupo de Electrónica Aplicada (GEA), Facultad de Ingeniería, Universidad Nacional de Río Cuarto, X5804BYA Río Cuarto, Argentina (e-mail: cdeangelo@ieee.org; gbossio@ing.unrc.edu.ar; g.garcia@ieee.org).

J. Solsona is with the Consejo Nacional de Investigaciones Científicas y Técnicas (CONICET), Argentina, and also with the Departamento de Ingeniería Eléctrica y de Computadoras, Instituto de Investigaciones en Ingeniería Eléctrica "Alfredo Desages," Universidad Nacional del Sur, 8000 Bahía Blanca, Argentina (e-mail: jsolsona@uns.edu.ar).

M. I. Valla is with the Consejo Nacional de Investigaciones Científicas y Técnicas (CONICET), Argentina, and also with the Laboratorio de Electrónica Industrial, Control e Instrumentación (LEICI), Departamento de Electrotecnia, Facultad de Ingeniería, Universidad Nacional de La Plata, 1900 La Plata, Argentina (e-mail: m.i.valla@ieee.org).

Digital Object Identifier 10.1109/TIE.2005.847582

improves the torque ripple reduction when compared with sinusoidal EMF-based observers.

This paper is organized as follows. In Section II, the PMACM general model is presented. In Section III, the proposed observer is developed. Section IV deals with some implementation aspects. In Section V, the proposal is validated with experimental results obtained by an axial-flux PMACM drive prototype. Finally, some conclusions are drawn in Section VI.

II. PMACM Model

In order to develop the proposed observer, the dynamic model of a PMACM is written in a stationary reference frame $\alpha\beta$ [8]

$$\begin{aligned} \frac{di_\alpha}{dt} &= -\frac{R}{L}i_\alpha - \frac{1}{L}e_\alpha + \frac{1}{L}v_\alpha \\ \frac{di_\beta}{dt} &= -\frac{R}{L}i_\beta - \frac{1}{L}e_\beta + \frac{1}{L}v_\beta \end{aligned} \tag{1}$$

$$\begin{aligned} \frac{d\theta}{dt} &= \omega \\ \frac{d\omega}{dt} &= \frac{1}{J}T_e - \frac{B}{J}\omega - \frac{1}{J}T_L \end{aligned} \tag{2}$$

where $i_\alpha, i_\beta, e_\alpha, e_\beta, v_\alpha, v_\beta$ represent the current, induced EMF, and excitation voltage components, respectively, in the stationary reference frame $\alpha\beta$; R and L are the stator resistance and inductance, respectively; θ, ω, and T_e represent the rotor position and speed, and the electromagnetic torque produced by the machine; J and B are the inertia and viscosity, respectively; and T_L is the load torque.

The EMF induced into the stator windings is given by

$$\begin{aligned} e_\alpha &= \frac{\partial\lambda_\alpha}{\partial\theta}\frac{d\theta}{dt} = \varphi_\alpha(\theta)\omega \\ e_\beta &= \frac{\partial\lambda_\beta}{\partial\theta}\frac{d\theta}{dt} = \varphi_\beta(\theta)\omega \end{aligned} \tag{3}$$

where λ_α and λ_β are the linked flux components, and φ_α and φ_β are the components of the flux derivative with respect to the rotor position.

In a sinusoidal PMACM, φ_α and φ_β are sinusoidal functions of the position whereas in trapezoidal PMACMs they are trapezoidal. However, in many PMACMs, these functions are neither sinusoidal nor trapezoidal. For this reason φ_α and φ_β are functions to be determined according to the motor type. These functions can be previously determined in an experimental way by measuring the instantaneous voltage, rotor position and speed under no-load condition, or by means of a self-commissioning scheme, as proposed in [9]. To include these waveforms in the PMACM model, a Fourier series approximation is used.

The $\alpha\beta$ components of the position derivatives of flux can be represented using Fourier series as follows:

$$\begin{aligned} \varphi_\alpha(\theta) &= \sum_{n=1}^{\infty} -\Phi_{(2n-1)}\sin((2n-1)\theta) \\ \varphi_\beta(\theta) &= \sum_{n=1}^{\infty} \Phi_{(2n-1)}\cos((2n-1)\theta) \end{aligned} \tag{4}$$

where $\Phi_{(2n-1)}$ is the magnitude of the $(2n-1)$ harmonic.

The electromagnetic torque in the last equation of (2) is given by [8]

$$T_e = \varphi_\alpha(\theta)i_\alpha + \varphi_\beta(\theta)i_\beta \tag{5}$$

so it is evident that in order to obtain a smooth controlled torque the excitation current waveforms greatly depend on the functions φ_α and φ_β.

The model presented in this section is not limited to sinusoidal or trapezoidal PMACMs. Based on this model, a nonlinear observer to estimate the induced EMF, the rotor position and the rotor speed for arbitrary EMF waveform PMACMs is introduced in the next section.

III. Nonlinear Observer

The information of speed and rotor position is contained in the induced EMF, as shown in (3). Therefore, it could be possible to estimate the induced EMF by measuring currents and voltages, and then calculate the motor speed and rotor position from the estimated EMF. In order to do that, the time derivative of EMF can be calculated from (3)

$$\begin{aligned} \frac{de_\alpha}{dt} &= \frac{d\varphi_\alpha}{dt}\omega + \varphi_\alpha\frac{d\omega}{dt} \\ \frac{de_\beta}{dt} &= \frac{d\varphi_\beta}{dt}\omega + \varphi_\beta\frac{d\omega}{dt}. \end{aligned} \tag{6}$$

From (6), the following EMF observer can be proposed:

$$\begin{aligned} \frac{d\hat{e}_\alpha}{dt} &= \frac{d\hat{\varphi}_\alpha}{dt}\hat{\omega} + \hat{\varphi}_\alpha\frac{d\hat{\omega}}{dt} + g\left(L\frac{d\hat{i}_\alpha}{dt} - L\frac{di_\alpha}{dt}\right) \\ \frac{d\hat{e}_\beta}{dt} &= \frac{d\hat{\varphi}_\beta}{dt}\hat{\omega} + \hat{\varphi}_\beta\frac{d\hat{\omega}}{dt} + g\left(L\frac{d\hat{i}_\beta}{dt} - L\frac{di_\beta}{dt}\right) \end{aligned} \tag{7}$$

where $\hat{x}$ is the estimated value of x, and the time derivatives of stator currents are used as correction terms. An appropriate gain g must be chosen when adjusting the observer in order to obtain desired convergence as shown in [3] (see Section IV).

The estimated current derivatives, necessary for obtaining the correction term, can be calculated with (1)

$$\begin{aligned} \frac{d\hat{i}_\alpha}{dt} &= -\frac{R}{L}i_\alpha - \frac{1}{L}\hat{e}_\alpha + \frac{1}{L}v_\alpha \\ \frac{d\hat{i}_\beta}{dt} &= -\frac{R}{L}i_\beta - \frac{1}{L}\hat{e}_\beta + \frac{1}{L}v_\beta. \end{aligned} \tag{8}$$

Furthermore, the time derivative of the estimated speed (acceleration, $\hat{a}$) used in (7) can be obtained from (2) and (5), assuming that no load torque exists ($T_L = 0$),

$$\hat{a} = \frac{d\hat{\omega}}{dt} = \frac{1}{J}(\hat{\varphi}_\alpha i_\alpha + \hat{\varphi}_\beta i_\beta) - \frac{B}{J}\hat{\omega}. \tag{9}$$

The estimate of the machine's speed can be found taking into account (3), so

$$e_\alpha^2 + e_\beta^2 = \omega^2\left(\varphi_\alpha^2 + \varphi_\beta^2\right), \tag{10}$$

and

$$\hat{\omega} = \sqrt{\frac{\hat{e}_\alpha^2 + \hat{e}_\beta^2}{\hat{\varphi}_\alpha^2 + \hat{\varphi}_\beta^2}}. \tag{11}$$

The calculation of the measured current derivative, used in the correction term (7), may end up in a noisy estimation. To avoid that, the following change of variables is proposed:

$$\begin{aligned}\hat{\zeta}_\alpha &= \hat{e}_\alpha + gLi_\alpha \\ \hat{\zeta}_\beta &= \hat{e}_\beta + gLi_\beta.\end{aligned} \tag{12}$$

Taking the time derivative of (12), and substituting from (7) and (8), the proposed observer will result in

$$\begin{aligned}\frac{d\hat{\zeta}_\alpha}{dt} &= \frac{d\hat{\varphi}_\alpha}{dt}\hat{\omega} + \hat{\varphi}_\alpha\hat{a} + g(-Ri_\alpha - \hat{e}_\alpha + v_\alpha) \\ \frac{d\hat{\zeta}_\beta}{dt} &= \frac{d\hat{\varphi}_\beta}{dt}\hat{\omega} + \hat{\varphi}_\beta\hat{a} + g(-Ri_\beta - \hat{e}_\beta + v_\beta)\end{aligned} \tag{13}$$

and the estimated EMF can be obtained by solving (12)

$$\begin{aligned}\hat{e}_\alpha &= \hat{\zeta}_\alpha - gLi_\alpha \\ \hat{e}_\beta &= \hat{\zeta}_\beta - gLi_\beta.\end{aligned} \tag{14}$$

This observer can be applied to any PMACM, independently of its EMF waveform. The only requirement for its implementation is to know the waveforms of the flux derivative with respect to the rotor position. These functions are incorporated in the observer by evaluating (4) in the estimated rotor position. Taking into account that the EMF waveform has several harmonic components, the estimated position can be calculated from the EMF fundamental, using

$$\hat{\theta} = \tan^{-1}\left(\frac{-\hat{e}_{\alpha 1}}{\hat{e}_{\beta 1}}\right) \tag{15}$$

where $e_{\alpha 1}, e_{\beta 1}$ are the induced EMF waveform fundamental components, which can be obtained by eliminating the harmonic components, as proposed in [10]. These harmonic components can be calculated at sample (k) from Fourier series approximation (4), evaluated in an approximation of the current position $\tilde{\theta}_{(k)}$. In order to do that, constant speed between two consecutive samples is considered, then,

$$\begin{aligned}\tilde{e}_{\alpha h(k)} &= \hat{\omega}_{(k-1)} \sum_{n=2}^{\infty} -\Phi_{(2n-1)} \sin\left((2n-1)\tilde{\theta}_{(k)}\right) \\ \tilde{e}_{\beta h(k)} &= \hat{\omega}_{(k-1)} \sum_{n=2}^{\infty} \Phi_{(2n-1)} \cos\left((2n-1)\tilde{\theta}_{(k)}\right)\end{aligned} \tag{16}$$

where $\tilde{e}_{\alpha h(k)}, \tilde{e}_{\beta h(k)}$ are the harmonic components of the estimated EMF (note that the sum is taken from $n = 2$).

The approximation of the current position is obtained considering the speed as

$$\tilde{\omega} = \frac{\theta_{(k)} - \theta_{(k-1)}}{T_s} \tag{17}$$

in a sample time T_s, so,

$$\tilde{\theta}_{(k)} = \hat{\theta}_{(k-1)} + \hat{\omega}_{(k-1)}T_s. \tag{18}$$

Then, the induced EMF fundamental components can be calculated subtracting the harmonic components (16) from the EMF estimated by the observer (14)

$$\begin{aligned}\hat{e}_{\alpha 1} &= \hat{e}_\alpha - \tilde{e}_{\alpha h(k)} \\ \hat{e}_{\beta 1} &= \hat{e}_\beta - \tilde{e}_{\beta h(k)}\end{aligned} \tag{19}$$

and the new estimated position is calculated from (15). Then, the estimated position derivative of flux is obtained as

$$\begin{aligned}\hat{\varphi}_\alpha(\hat{\theta}) &= \sum_{n=1}^{\infty} -\Phi_{(2n-1)} \sin((2n-1)\hat{\theta}) \\ \hat{\varphi}_\beta(\hat{\theta}) &= \sum_{n=1}^{\infty} \Phi_{(2n-1)} \cos((2n-1)\hat{\theta})\end{aligned} \tag{20}$$

and their estimated time derivatives can be calculated as

$$\begin{aligned}\frac{d\hat{\varphi}_\alpha}{dt} &= \hat{\omega} \sum_{n=1}^{\infty} -(2n-1)\Phi_{(2n-1)} \cos((2n-1)\hat{\theta}) \\ \frac{d\hat{\varphi}_\beta}{dt} &= \hat{\omega} \sum_{n=1}^{\infty} -(2n-1)\Phi_{(2n-1)} \sin((2n-1)\hat{\theta})\end{aligned} \tag{21}$$

which completes the proposed observer for PMACMs with arbitrary EMF waveform.

IV. Implementation

The observer proposed in Section III shows the same indistinguishability problems as all those that use currents or their derivatives in the correction term [3]. Therefore, the sign of the speed cannot be obtained from (11). Therefore, in a practical implementation, the speed sign can be obtained from the sign of the time derivative of the estimated position $(d\hat{\theta}/dt \approx (\hat{\theta}_{(k)} - \hat{\theta}_{(k-1)})/T_s)$.

Another implementation aspect is the calculus of the functions that are approximated by Fourier series. Although the observer was developed using infinite series, harmonics greater than 12 or 15 are generally small, and their contribution to the torque ripple is insignificant [7]. Therefore, Fourier series approximations used in the implementation are considered from $n = 1$ to $n = N$, in such a way that $2N - 1$ is the maximum harmonic considered.

Truncation of the Fourier series introduces a nonvanishing perturbation in the estimation error dynamics. This causes the nonconvergence of the error to zero; indeed, it will be ultimately bounded by a small bound [11, ch. 5]. The ultimate bound value can be reduced either by increasing the number of harmonics or by increasing the gain g. Also, the observer gain g must correctly be chosen to guarantee the stability of the control system when using the estimated variables in a sensorless control strategy. Using a singular perturbation argument [11, ch. 9], observer and control dynamics can be separated if gain g is chosen high enough to ensure the observer dynamics faster than the control dynamics. In this case, if the observer converges quickly enough, the control system using the estimated variables could be approximated by a system without the observer. However, the maximum value of g is limited by the influence of the measurement noise. Then, the selection of gain g results from a tradeoff

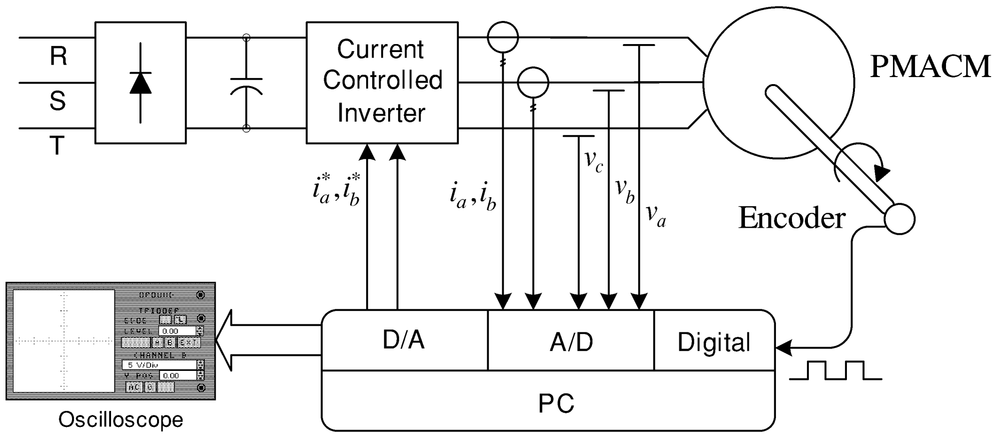

Fig. 1. Experimental setup.

between observer convergence speed and measurement noise as will be shown with the experimental results.

Finally, considering the previously stated equations, the observer algorithm can be implemented as follows:

- *initial conditions:* $\hat{\theta}(0), \hat{\omega}(0)$
- *inputs:* $i_\alpha, i_\beta, v_\alpha, v_\beta$
- *algorithm:*

$$\hat{\varphi}_\alpha(\hat{\theta}) = \sum_{n=1}^{N} -\Phi_{(2n-1)} \sin((2n-1)\hat{\theta})$$
$$\hat{\varphi}_\beta(\hat{\theta}) = \sum_{n=1}^{N} \Phi_{(2n-1)} \cos((2n-1)\hat{\theta}) \tag{22}$$
$$\frac{d\hat{\varphi}_\alpha}{dt} = \hat{\omega} \sum_{n=1}^{N} -(2n-1)\Phi_{(2n-1)} \cos((2n-1)\hat{\theta})$$
$$\frac{d\hat{\varphi}_\beta}{dt} = \hat{\omega} \sum_{n=1}^{N} -(2n-1)\Phi_{(2n-1)} \sin((2n-1)\hat{\theta}) \tag{23}$$
$$\hat{a} = \frac{1}{J}(\hat{\varphi}_\alpha i_\alpha + \hat{\varphi}_\beta i_\beta) - \frac{B}{J}\hat{\omega} \tag{24}$$
$$\frac{d\zeta_\alpha}{dt} = \frac{d\hat{\varphi}_\alpha}{dt}\hat{\omega} + \hat{\varphi}_\alpha \hat{a} + g(-Ri_\alpha - \hat{e}_\alpha + v_\alpha)$$
$$\frac{d\zeta_\beta}{dt} = \frac{d\hat{\varphi}_\beta}{dt}\hat{\omega} + \hat{\varphi}_\beta \hat{a} + g(-Ri_\beta - \hat{e}_\beta + v_\beta) \tag{25}$$
$$\hat{e}_\alpha = \zeta_\alpha - gLi_\alpha$$
$$\hat{e}_\beta = \zeta_\beta - gLi_\beta \tag{26}$$
$$\tilde{\theta}_{(k)} = \hat{\theta}_{(k-1)} + \hat{\omega}_{(k-1)} T_s \tag{27}$$
$$\tilde{e}_{\alpha h(k)} = \hat{\omega}_{(k-1)} \sum_{n=2}^{N} -\Phi_{(2n-1)} \sin\left((2n-1)\tilde{\theta}_{(k)}\right)$$
$$\tilde{e}_{\beta h(k)} = \hat{\omega}_{(k-1)} \sum_{n=2}^{N} \Phi_{(2n-1)} \cos\left((2n-1)\tilde{\theta}_{(k)}\right) \tag{28}$$
$$\hat{e}_{\alpha 1} = \hat{e}_\alpha - \tilde{e}_{\alpha h(k)}$$
$$\hat{e}_{\beta 1} = \hat{e}_\beta - \tilde{e}_{\beta h(k)} \tag{29}$$
$$\hat{\theta} = \tan^{-1}\left(\frac{-\hat{e}_{\alpha 1}}{\hat{e}_{\beta 1}}\right) \tag{30}$$
$$\hat{\omega} = \text{sign}\left(\frac{\hat{\theta}_{(k)} - \hat{\theta}_{(k-1)}}{T_s}\right)\sqrt{\frac{\hat{e}_\alpha^2 + \hat{e}_\beta^2}{\hat{\varphi}_\alpha^2 + \hat{\varphi}_\beta^2}}. \tag{31}$$

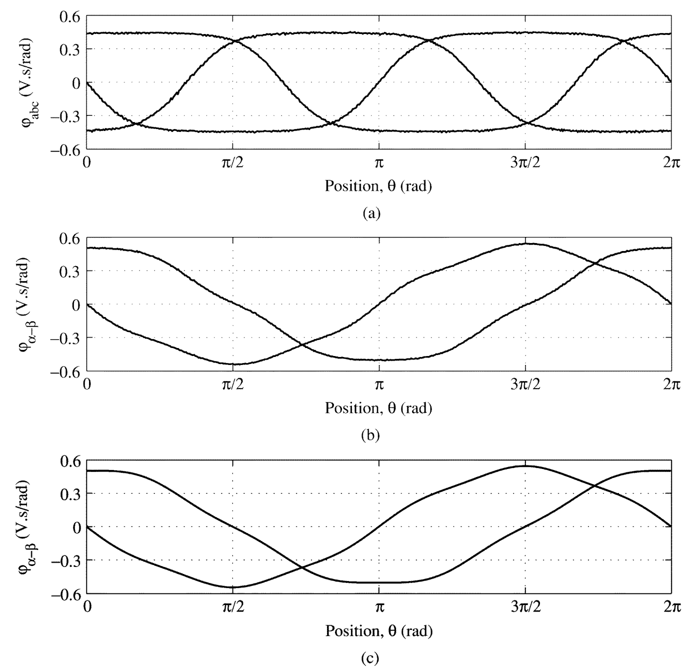

Fig. 2. Position derivative of linked flux versus rotor position (in electrical radians). (a) For each phase. (b) In $\alpha\beta$ coordinates. (c) Fourier series approximation.

V. Experimental Results

Fig. 1 shows the experimental setup that was used to validate the proposed observer. The motor is an experimental prototype of an axial-flux PMACM [12], driven by a pulsewidth-modulated inverter with a fast current control loop, available at the laboratory of the Grupo de Electrónica Aplicada, Universidad Nacional de Río Cuarto, Río Cuarto, Argentina. The motor parameters are a follows:

three-phase axial-flux permanent-magnet motor, 16 poles, 4000 r/min, 30 kW;
$R = 10$ mΩ;
$L = 100$ μH;
$J = 0.78$ kg·m^2;
$B = 0.0015$ kg·m^2/s.

Fig. 2(a) shows the experimentally determined waveforms of the position derivatives of flux versus rotor position (induced

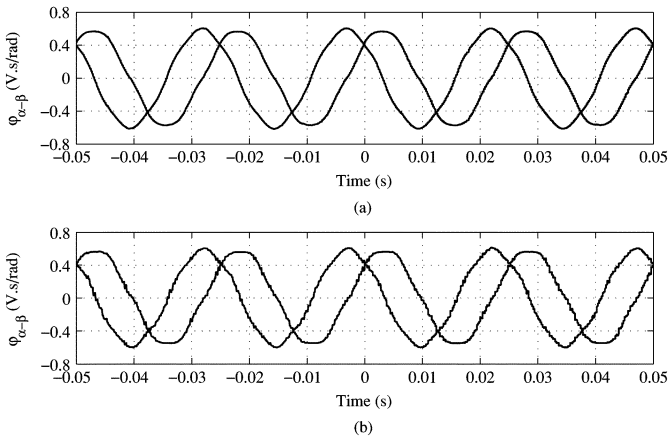

Fig. 3. Position derivative of linked flux at low speed. (a) Measured. (b) Estimated.

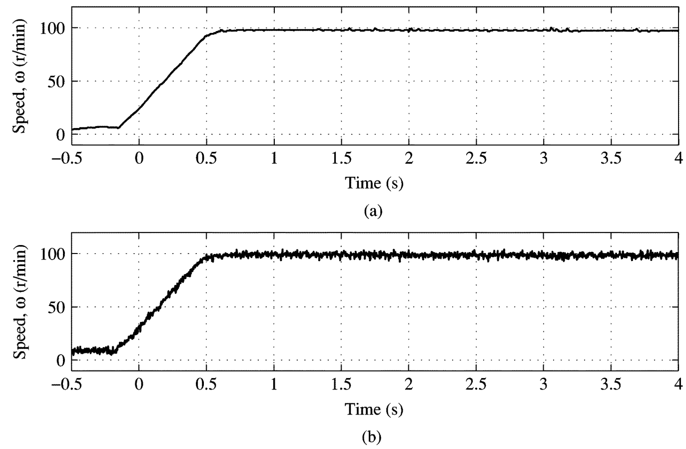

Fig. 4. Rotor speed at low speed. (a) Measured. (b) Estimated.

EMF divided by speed). The position derivative of flux components in $\alpha\beta$ coordinates is needed to implement the observer. These functions are shown in Fig. 2(b). A good approximation of these waveforms, using Fourier series, can be obtained with only two terms ($\Phi_1 = 0.5021$, and $\Phi_5 = \Phi_1/25$), as shown in Fig. 2(c).

The proposed observer was implemented using a PC, running the algorithm presented in Section IV, programmed in C++ language. Differential equations were discretized using the Euler method with sampling period equal to 200 μs. Motor voltages and currents were measured using standard Hall-effect sensors and acquired by means of 12-b A/D converters. The observer gain was set at 800.

A. Proposed Observer

Experimental results showing how the proposed observer works are presented here. First of all, the drive speed control loop was closed by the measured variables, using a 1024–pulse encoder. Measured data are compared with the estimated data in order to validate the observer.

Fig. 3(b) shows the estimation of the position derivative of flux in $\alpha\beta$ coordinates, when the motor runs at low speed, 300 r/min (0.075 p.u.). The waveforms shown here are a very good estimation of the actual ones presented in Fig. 3(a).

A low-speed test is presented in Fig. 4. The unloaded motor is running at 100 r/min (0.025 p.u.) when a sudden change in the reference speed occurs. The estimated and actual speeds are shown in Fig. 4(a) and (b), respectively. The estimated speed shows some ripple, which is the consequence of the noisy measurements and the observer gain. This ripple may be improved by either reducing the observer gain or improving the measurements.

Position estimation at low speed is shown in Fig. 5. In Fig. 5(a) the actual rotor position at 100 r/min (0.025 p.u.) is shown. The estimated position is shown in Fig. 5(b), while the estimation position error ($\varepsilon_\theta = \theta - \hat{\theta}$) is presented in Fig. 5(c).

A speed reversal test is shown in Fig. 6. It can be seen that the speed sign cannot be precisely determined at low speed, due to the above-mentioned measurement noise.

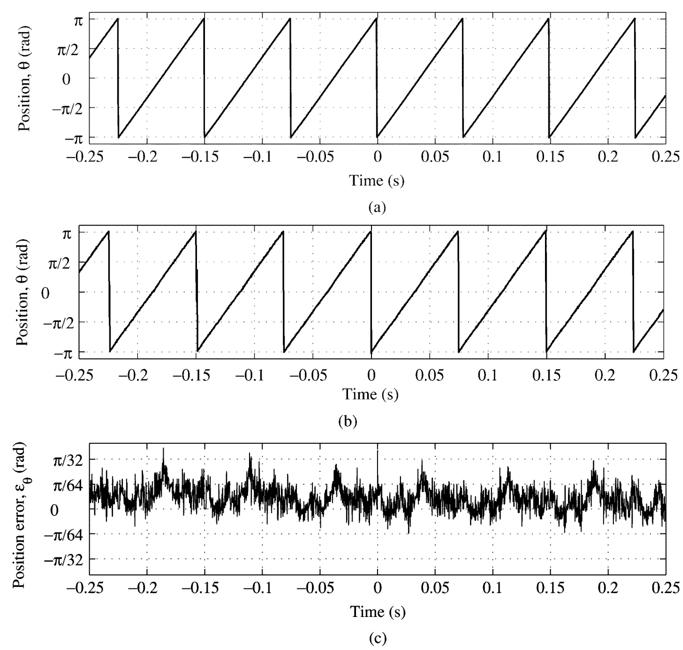

Fig. 5. Rotor position (in electrical radians) at low speed. (a) Measured. (b) Estimated. (c) Estimation position error.

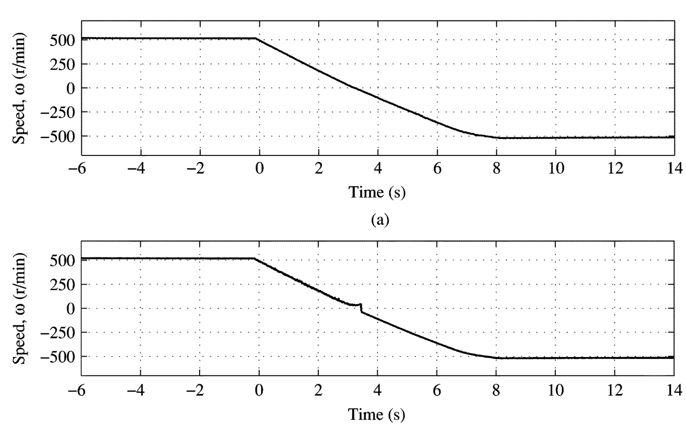

Fig. 6. Rotor speed during speed reversal. (a) Measured. (b) Estimated.

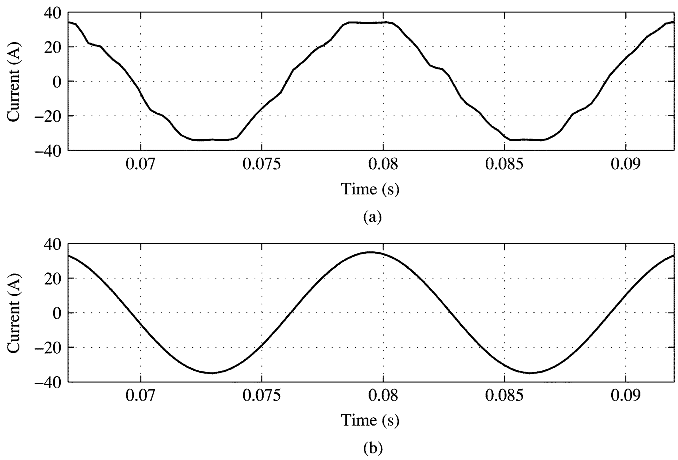

Fig. 7. "Offline" calculation of the phase-a current reference. (a) With the proposed observer. (b) With an observer with sinusoidal EMF.

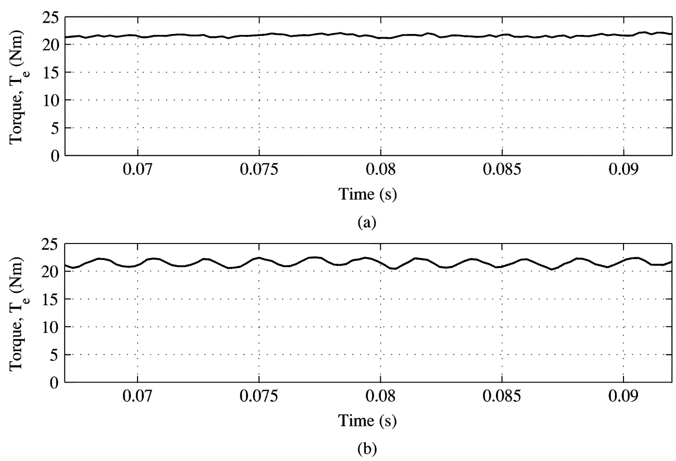

Fig. 8. "Offline" calculation of the motor torque using (a) the proposed observer and (b) an observer with sinusoidal EMF.

B. Comparison Between the Proposed Observer and a Sinusoidal One

As mentioned in Section I, a popular approach to reduce torque ripple is the PCWC technique. In this technique, excitation currents are generated as functions of the EMF waveform, synchronized with the rotor position [7]. The proposed observer can be used with a PCWC technique in order to minimize the torque ripple in a sensorless PMACM drive, avoiding the use of a mechanical position sensor.

In order to validate this application, the observer was used to calculate the excitation currents together with the PCWC scheme proposed in [13], which allows the reduction of the motor torque ripple, provided that the functions φ_α and φ_β are well known or estimated. Current references were calculated as in [13], using the estimated position derivatives of flux [shown in Fig. 3(b)]. Fig. 7(a) shows the calculated current references using the proposed observer. If a sinusoidal EMF distribution is supposed, sinusoidal current references will be generated, as shown in Fig. 7(b). With these currents and the experimentally determined position derivative of flux [Fig. 2(b)], the electromagnetic torque can be calculated using (5). The result of this "offline" calculation with both current waveforms is shown in Fig. 8. As can be seen, the use of the proposed observer greatly reduces the torque ripple with respect to a conventional sinusoidal approximation.

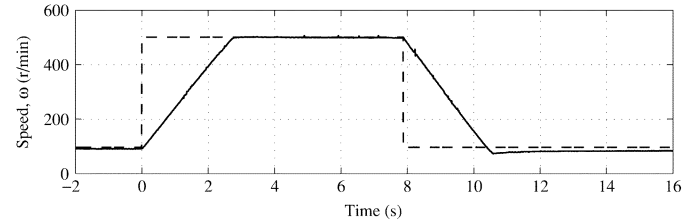

Fig. 9. Speed reference (dashed line) and measured speed (solid line).

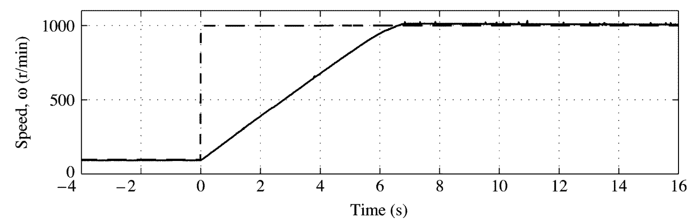

Fig. 10. Speed reference (dashed line) and measured speed (solid line).

C. Application of the Proposed Observer in a Closed-Loop Sensorless Drive

Experimental results using the proposed observer in a sensorless speed control strategy are presented in this section. The estimated variables are used to close the torque and speed control loops in the experimental drive.

In Figs. 9 and 10, reference speed (dashed line) and measured speed (solid line) are shown for different operating conditions. In Fig. 9, sensorless operation in the low-speed range is presented. Reference speed is changed from 100 r/min (0.025 p.u.) to 500 r/min (0.125 p.u.), and to 100 r/min again, at 8 s. Even when operation at lower speed is possible, speed estimation is affected by measurement noise in this speed range. Fig. 10 shows motor operation from low speed (100 r/min) to high speed (1000 r/min).

As can be seen, closed-loop system operation using the estimated variables is satisfactory in a wide speed range.

VI. Conclusion

A new nonlinear reduced-order observer to estimate the rotor speed and position for permanent-magnet motors has been proposed in this paper. Unlike previous proposals, this observer is not limited to sinusoidal or trapezoidal PMACMs. Indeed, the observer allows the estimation of the induced EMF with arbitrary waveforms. Consequently, this proposal, used together with a programmed current waveform control strategy, represents an advantageous option for the realization of a torque controller with minimum torque ripple.

The proposed observer was used to implement a sensorless PMACM drive prototype, with torque ripple minimization. Experimental results confirm the good performance of the observer in the estimation of EMF as well as rotor speed and position.

REFERENCES

[1] T. M. Jahns, "Variable frequency permanent magnet AC machine drives," in *Power Electronics and Variable Frequency Drives*, B. K. Bose, Ed. New York: IEEE Press, 1997, pp. 277–331.

[2] J. Johnson, M. Ehsani, and Y. Güzelgünler, "Review of sensorless methods for brushless DC," in *Conf. Rec. IEEE-IAS Annu. Meeting*, vol. 1, Phoenix, AZ, Oct. 3–7, 1999, pp. 143–150.

[3] J. Solsona, M. I. Valla, and C. Muravchik, "A nonlinear reduced order observer for permanent magnet synchronous motors," *IEEE Trans. Ind. Electron.*, vol. 43, no. 4, pp. 492–497, Aug. 1996.

[4] Y. Kim and Y. Kook, "High performance IPMSM drives without rotational position sensors using reduced-order EKF," *IEEE Trans. Energy Convers.*, vol. 14, no. 4, pp. 868–873, Dec. 1999.

[5] J. C. Moreira, "Indirect sensing for rotor flux position of permanent magnet AC motors operating over a wide speed range," *IEEE Trans. Ind. Appl.*, vol. 32, no. 6, pp. 1394–1401, Nov./Dec. 1996.

[6] S. Ogasawara and H. Akagi, "An approach to position sensorless drive for brushless DC motors," *IEEE Trans. Ind. Appl.*, vol. 27, no. 5, pp. 928–933, Sep./Oct. 1991.

[7] T. Jahns and W. Soong, "Pulsating torque minimization techniques for permanent magnet AC motor drives—A review," *IEEE Trans. Ind. Electron.*, vol. 43, no. 2, pp. 321–330, Apr. 1996.

[8] R. Krishnan, *Electric Motor Drives: Modeling, Analysis, and Control*. Upper Saddle River, NJ: Prentice-Hall, 2001.

[9] J. Holtz and L. Springob, "Identification and compensation of torque ripple in high-precision permanent magnet motor drives," *IEEE Trans. Ind. Electron.*, vol. 43, no. 2, pp. 309–320, Apr. 1996.

[10] M. Degner and R. Lorenz, "Using multiple saliencies for the estimation of flux, position, and velocity in AC machines," *IEEE Trans. Ind. Appl.*, vol. 34, no. 5, pp. 1097–1104, Sep./Oct. 1998.

[11] H. K. Khalil, *Nonlinear Systems*, 2nd ed. Englewood Cliffs, NJ: Prentice-Hall, 1996.

[12] A. Agüero, P. Zanello, V. Campra, L. Zanello, C. Candiani, R. Leidhold, and G. García, "Accionamiento para Tracción Eléctrica: Motor de flujo axial," in *An. VIII Reunión de Trabajo en Procesamiento de la Información y Control (VIII RPIC)*, vol. 1, Mar del Plata, Argentina, Sep. 23–25, 1999, pp. 89-2–95-2.

[13] R. Leidhold, G. García, and E. Watanabe, "PMAC motor control strategy, based on the instantaneous active and reactive power, for ripple-torque and copper-losses minimization," in *Proc. IEEE IECON'00*, vol. 2, Nagoya, Japan, Oct. 22–28, 2000, pp. 1401–1405.

Cristian De Angelo (S'96–M'05) received the Electrical Engineer degree from the Universidad Nacional de Río Cuarto, Río Cuarto, Argentina, in 1999, and the Dr. of Engineering degree from the Universidad Nacional de La Plata, La Plata, Argentina, in 2004.

In 1994, he joined the Grupo de Electrónica Aplicada (GEA), Universidad Nacional de Río Cuarto. He is also currently with the Consejo Nacional de Investigaciones Científicas y Técnicas (CONICET). His research interests are in power electronics, sensorless motor control, electric vehicles, and renewable energy generation.

Dr. De Angelo is a Member of the Automatic Control Association of Argentina (AADECA).

Guillermo Bossio received the Electrical Engineer degree from the Universidad Nacional de Río Cuarto, Río Cuarto, Argentina, in 1999, and the Dr. of Engineering degree from the Universidad Nacional de La Plata, La Plata, Argentina, in 2004.

In 1994, he joined the Grupo de Electrónica Aplicada (GEA), Universidad Nacional de Río Cuarto. He is also currently with the Consejo Nacional de Investigaciones Científicas y Técnicas (CONICET). His research interests are in power electronics, sensorless motor control, electric vehicles, and renewable energy generation.

Dr. Bossio is a Member of the Automatic Control Association of Argentina (AADECA).

Jorge Solsona (S'94–M'96–SM'04) received the Electronics Engineer and Doctor of Engineering degrees from the Universidad Nacional de La Plata, La Plata, Argentina, in 1986 and 1995, respectively.

From 1987 to 1997, he was a Member of the Industrial Electronics, Control and Instrumentation Laboratory, Departamento de Electrotecnia, Facultad de Ingeniería, Universidad Nacional de La Plata. He was with the Departamento de Electrotecnia, Facultad de Ingeniería, Universidad Nacional del Comahue, between 1997–2003. Currently, he is with the Instituto de Investigaciones en Ingeniería Eléctrica "Alfredo Desages," Departamento de Ingeniería Eléctrica y Computadoras, Universidad Nacional del Sur, Bahía Blanca, Argentina, and also with the Consejo Nacional de Investigaciones Científicas y Técnicas (CONICET). He is involved in teaching and research in control theory and its applications to electromechanical systems.

Dr. Solsona is a Member of the Automatic Control Association of Argentina (AADECA).

Guillermo O. García (M'86–SM'01) received the Electrical and Electronics Engineering degree from the Universidad Nacional de Córdoba, Córdoba, Argentina, in 1981, and the M.Sc. and Dr. degrees in electrical engineering from COPPE, Universidade Federal do Rio de Janeiro, Rio de Janeiro, Brazil, in 1990 and 1994, respectively.

In 1994, he joined the Universidad Nacional de Río Cuarto (UNRC), Río Cuarto, Argentina. Currently, he is Director of the Grupo de Electrónica Aplicada (GEA), Coordinator of the Graduate Program in Electrical Engineering, and a Professor at the Electrical and Electronics Engineering Department, UNRC. He is also with the Consejo Nacional de Investigaciones Científicas y Técnicas (CONICET). His research interests are in power electronics, motion control, electric vehicles, and renewable energy conversion.

Dr. García is a Member of the Automatic Control Association of Argentina (AADECA).

María Inés Valla (S'79–M'80–SM'97) received the Electronics Engineering and Doctor of Engineering degrees from the National University of La Plata (UNLP), Argentina, in 1980 and 1994, respectively.

Currently, she is a Full Professor in the Departamento de Electrotecnia, Facultad de Ingeniería, UNLP. She is also with the Consejo Nacional de Investigaciones Científicas y Técnicas (CONICET). She is engaged in teaching and research in the areas of power converters and ac motor drives.

Dr. Valla is a Member of the AdCom of the IEEE Industrial Electronics Society (IES) and the IES Coordinator of Membership for Region 9. She has been a member of the organizing committees of several international conferences. She is also a Member of the Argentina Automatic Control Association (AADECA).